Journal of the Nivar Volume 49, Special Issue, Autumn 2025 and Winter 2026, P. 41-59

Homepage: https://nivar.irimo.ir (Research Article)

Forecasting short-term precipitation using artificial intelligence on the southern coast of the Caspian Sea

Donya Sadeghnezhad [1]✉ | Ebrahim Fattahi [2] | Gholamali Kamali [3] Zahra Ghassabi [4] Majid Vazife Doust [5]

1. Corresponding Author, Doctoral student of Meteorology, Islamic Azad University, Science and Research Unit, Tehran, Iran.
2. Associate Professor of Climatology, Research Institute of Meteorology and Atmospheric Sciences, Tehran, Iran.
3. Associate Professor of Climatology, Islamic Azad University, Science and Research Unit, Tehran, Iran.
4. Assistant Professor of Meteorology, Research Institute of Meteorology and Atmospheric Sciences, Tehran, Iran.
5 Assistant Professor of Water Engineering, Gilan University, Gilan, Iran.

Corresponding Author E-mail: donyasadeghnezhad@gmail.com

(Received: 08 Apr 2025, Revised: 05 May 2025, Accepted: 12 May 2025, Published online: 23 Sep 2025)

Abstract

Rainfall is considered one of the most important input data for hydrological systems, and studying and measuring it is often necessary for runoff, groundwater, flooding, and sediment studies. Traditionally, rainfall measurement is conducted using rain gauges. Rain gauges are the most reliable source of rainfall observations and are used in most studies as a reference for comparing and validating satellite data. However, they have limited and irregular spatial coverage. In recent decades, advancements in remote sensing technologies for rainfall have led to a significant reduction in the chronic lack of spatial information, making vast datasets on precipitation available with unprecedented resolution in both space and time today, various meteorological satellites such as TRMM, ERA5, CHIRPS, and GPM are actively monitoring the Earth's atmospheric conditions, cloud cover, and humidity, with a high spatial resolution of around kilometers. Precipitation maps from these datasets have been continuously and consistently available on a global scale, but the resulting output images have a low spatial resolution of 25×25 kilometers. This spatial resolution is not highly applicable in small basins and irrigation and drainage networks. In this study, in order to develop an algorithm to increase the spatial resolution of satellite-based precipitation products, an algorithm was extracted using downscaling methods SVM ,RF, KNN,GBR with the help of the relationship between the physical characteristics of clouds and precipitation. Between September 2018 and December 2018 and September 2019 to December 2019 on the GEE platform, precipitation data were downscaled to 1 kilometer using cloud physical properties and data downscaling methods. The downscaled data RF has a higher coefficient of determination and better agreement with ground station data.

Keywords: Machine learning model, Physical characteristics of the cloud, precipitation, Short-term forecast.

Cite this article: Sadeghnezhad,D. , Fattahi,E. , Kamali,G. , Ghassabi,Z. and Vazifedoust,M. (2025). Forecasting short-term precipitation using artificial intelligence on the southern coast of the Caspian Sea. (e236589). Journal of the Nivar, *49* (Special Issue (S1), e236589 doi: 10.30467/nivar.2025.521906.1335

E-mail: (2) ebfat2002@yahoo.com (3) a.kamali@srbiau.ac.ir (4) z.ghassabi@gmail.com (5) majid.vazifedoust@yahoo.com

Publisher: Iran Meteorological Organization
DOI: https://doi.org/10.30467/nivar. 2025.521906.1335

Print ISSN: 1735-0565
Online ISSN: 2645-3347

1. Introduction

Precipitation is one of the most important climatic parameters, and its accurate prediction has significant impacts on human society and natural ecosystems. General methods for predicting precipitation include station methods, telemetric systems, weather forecasting models, and remote sensing-based systems, each of which has its own limitations.One of the most common tools for measuring precipitation in most river basins is the use of rain sensors at ground stations, which are widely used in various parts of the world. However, due to the lack of a dense and organized network of meteorological stations for measuring and transmitting parameters in real-time after occurrence, the application of this method faces serious limitations.Another method for predicting these parameters is the use of telemetry-based systems, where after measuring the parameter from one or several stations far from the center, information is sent to the monitoring unit through a fully automated connection. Although with the new approach of the Meteorological Organization of the country, all synoptic stations are in the process of converting to automatic stations with the aim of creating an automatic monitoring network, due to the transmission of data at the time of the event, these pieces of information are practically not useful for timely prediction in small basins.Numerical weather prediction models that simulate systematic patterns of precipitation events with adequate accuracy through general circulation modeling, play a significant role in flood warning systems and reducing human and financial losses when combined with hydrological models, communication systems, and collaboration with local people. For example, we can refer to the flood warning systems in the Karun River Basin (Meteorological Research Institute, 2006), Golestan Province, and the flood warning system of selected basins in Gilan Province (Meteorological Research Institute, 2009), which combine predictive meteorological models of temperature and precipitation (for one to five days ahead with a six-hour time step), hydrological models (precipitation-runoff), and hydraulic models (flow routing in rivers). Some key variables such as the time, location, and intensity of flood flows can be predicted.However, low spatial resolution and simplification of real conditions have always been controversial challenges presented in numerical models. In addition, as spatial resolution increases, higher computational power is required. Temporal accuracy in numerical models is always approximate, such that the occurrence of convective phenomena cannot be precisely predicted at a specific time. Therefore, these models, due to their large scale, do not provide suitable accuracy in predicting convective rainfall and spring and summer precipitation, and only model systematic and bulk precipitation in the autumn and winter seasons with appropriate accuracy (Zayayan, 1396).In the monitoring and control of natural disasters, current precipitation forecasts rely heavily on numerical weather prediction (NWP), which is widely used in hydrological forecasting. However, given that precipitation is not a continuous variable and shows significant spatial and temporal variability, the inherent complexity and nonlinearity of atmospheric dynamic processes make short-term precipitation forecasting quite challenging.In recent years, medium-range weather prediction (NWP) systems have primarily been composed of the National Centers for Environmental Prediction (NCEP), the Global Forecasting System (GEFS), and the European Centre for Medium-Range Weather Forecasts (ECMWF) (Medina et. Al, 2019). (Liu et al., 2021). After categorizing precipitation into light, medium, and heavy based on threshold limits, the accuracy of the ECMWF model predictions for precipitation in the western Pacific region was analyzed. Their findings indicate that in the northern regions, the number of heavy instantaneous rain events that were not predicted is higher compared to the southern regions, while in the southwestern areas, the highest number of false alarms for heavy rainfall occurrences has been experienced. In another study, Lewis and colleagues (2017) examined the

results of the GEFS model in the western parts of the United States and showed that despite the relatively accurate predictions of the GEFS model in coastal areas, its performance decreases in inland regions, especially in high-elevation areas, indicating limitations in precipitation forecasting due to the topography of the land (Lewis et al., 2017).The above studies show that medium-term weather prediction systems face regional issues in forecasting precipitation. Different NWP models also vary in their performance and prediction accuracy in different areas. (Ran et al., 2018). The predictions of these models are influenced by improper initial conditions, numerical estimations, and simplifications of the physical and chemical processes governing the atmosphere. These shortcomings, approximations, and simplifications lead to random and systematic errors that greatly affect the accuracy of predictions. To reduce systematic errors, many post-processing approaches and data assimilation processes have been proposed (Monaesh and colleagues, 2011). Although classic weather prediction systems NWP can be effectively expanded through data assimilation techniques, this can be a time-consuming and costly process (Lewis et al., 2017).The predictions of these models are influenced by unsuitable initial conditions, numerical estimates, and simplifications of the physical and chemical processes governing the atmosphere. These deficiencies, approximations, and simplifications lead to the generation of random and systematic errors that significantly impact the accuracy of predictions. To reduce systematic errors, many post-processing approaches and data mining processes have been proposed (Monash et al., 2011).Although classic NWP weather prediction systems can be effectively enhanced through data assimilation and techniques, this can be a time-consuming and costly process. In comparison to the aforementioned NWP systems, due to the rapid development of machine learning-based techniques, their methods have been widely used for precipitation parameter forecasting and have achieved satisfactory forecasting results (Sachindra et al. 2018, Ahmed et al. 2020, Song et al. 2021, Senocak et al. 2023, Davenport et al. 2021).In addition, to manage a larger volume of data and tasks for forecasting time series trends, deep learning techniques are employed, which have advantages that classic machine learning and NWP systems face challenges in achieving. For example, the FourCastNet neural network is a global data-based weather prediction model capable of providing accurate short-term global forecasts with a resolution of 0.25. Compared to the ECMWF integrated forecasting system (IFS), FourCastNet not only matches the accuracy of the forecasts but also generates predictions for one week in less than 2 seconds, which is several times faster than IFS (Pathak et al. 2023). This is a very important distinction due to the nature of AI-ML compared to classic NWP models. GraphCast, a large-scale weather forecasting model developed by Google DeepMind Research, is a machine learning-based approach that is directly trained from reanalysis data. It predicts hundreds of weather variables for the next ten days with a resolution of 0.25 degrees within a minute. GraphCast outperforms the most accurate deterministic operational systems in 90 percent of validation targets (Lam et al. 2023). The Pangu-Weather LM developed by Bi et al. 2023, trained on 39 years of global data, has achieved stronger deterministic forecasting results across all tested variables compared to IFS ECMWF. The results demonstrate the superior performance of Pangu-Weather in predicting severe weather, with an operational speed 10,000 times faster than IFS. Therefore, generative artificial intelligence models, in addition to being used to quantify uncertainty in weather prediction, allow for the costly process to be diminished by using these models. Li and colleagues (2023) a convolutional neural network model and short-term memory (CNN-LSTM) Based on deep learning, a model was proposed for predicting 3-hour rainfall in the city of Lanzhou, achieving better predictive performance compared to classic machine learning methods. Rojas Campos and colleagues (2023) The superior performance of artificial

neural networks (ANN) It showed the estimation of the probability of precipitation and the prediction of hourly rainfall. Machine learning and deep learning have been widely used in precipitation forecasting. However, achieving accurate medium-term precipitation predictions remains a challenge.

2. Study Area

In this article, the possibility of predicting rainfall in the one to three-day time frame is examined using the analysis of heavy rainfall occurrence conditions and the utilization of data sources including the output of numerical weather prediction models, data and information obtained from meteorological satellites, historical station data, global land surface models, and the use of artificial intelligence-based methods. Ultimately, an advanced algorithm for predicting rainfall parameters along the coastal strip of the Caspian Sea is designed and developed using artificial intelligence-based methods. In this study, the ability of AI-based models to predict precipitation in the coastal strip of the Caspian Sea is evaluated using data sources including outputs from numerical prediction models, data and information obtained from meteorological satellites, historical station data, global land surface models, and also using actual values from stations as reference values for evaluation.

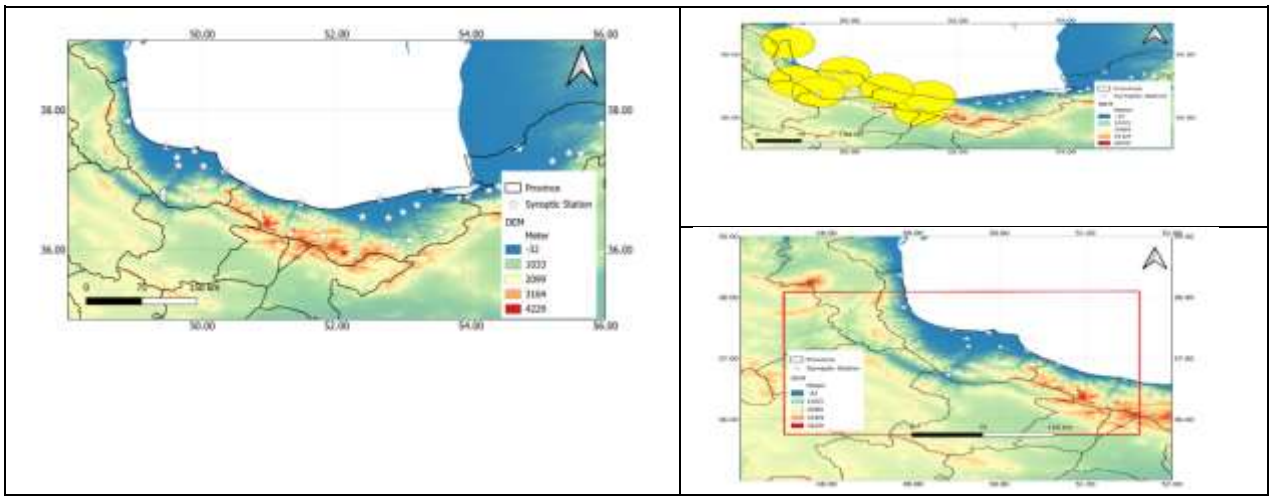

Figure 1 - The geographical location of the provinces of Gilan and Mazandaran in the north of Iran.

ML models including support vector machine (SVM), k-nearest neighbors (KNN), random forest (RF) and gradient boosting regressor (GBR) were trained and tested to estimate the water quality parameters in Anzali Wetland. The models were fine-tuned using a comprehensive hyperparameter grid search to optimize their performance. This systematic exploration of hyperparameters allowed for the identification of optimal configurations for each model, leading to robust estimations of water quality parameters.SVM models are supervised learning algorithms used for classification and regression tasks. SVM works by finding the optimal hyperplane that best separates data points from different classes in a high-dimensional space. For regression, SVM minimizes error within a margin of tolerance, known as epsilon. For the SVM models, the regularization parameter (C) was tuned using values of [0.1, 1, 10], while the epsilon was tested with [0.01, 0.1, 0.2]. Both linear and radial basis function (RBF) kernels were considered for the SVM models.KNN models predict the output based on the average of the nearest neighbors in feature space. This method is simple yet effective, particularly when the data exhibits clear clusters or patterns. The number of neighbors for the KNN models in the present study was varied between 3 and 11, with both uniform and distance-based weighting schemes used to optimize the KNN performance.RF models are ensemble learning

methods primarily used for classification and regression tasks. RF constructs a multitude of decision trees during training and aggregates their predictions to improve accuracy and reduce overfitting. Each tree in the forest is built from a random subset of the training data, which enhances the model's robustness. The RF models were fine-tuned by adjusting the number of decision trees from [50, 100, 200]. The maximum depth of the trees was either unrestricted or limited to [10, 20], and the minimum number of samples required to split a node was varied between [2, 5, 10].GBR models sequentially build a set of weak learners, typically decision trees, where each new tree attempts to correct the errors of the previous one. This iterative boosting process improves prediction accuracy. The GBR models were tested with a wide range of hyperparameters, including the number of boosting stages from [25, 50, 100, 200], learning rates from [0.01, 0.1, 0.2], and maximum tree depths set to [3, 5, 7, 9, 11, 13, 15].

3. Measurement,Observation, and Calculation (Reorganized and etailed)

This section details the diverse data sources utilized, the machine learning architectures employed, the rigorous evaluation metrics applied, and the characteristic ranges of the input parameters used in the precipitation forecasting models.

3.1. Data and Information Required The study employs a heterogeneous dataset integrating ground-truth measurements with large-scale atmospheric reanalysis products to provide a comprehensive view of meteorological conditions influencing precipitation.
Ground Truth and Reanalysis Data Sources

1. Ground Station Data (Reference Measurements)

Local meteorological station data provides high-resolution, point-specific measurements of actual precipitation, serving as the primary target variable for local model calibration and validation. These observations are crucial for assessing the localized skill of the developed forecasting models.

2. Global Forecast System (GFS)

GFS data, a global numerical weather prediction model output, provides the initial large-scale context for atmospheric dynamics, including boundary conditions and broad-scale atmospheric variables necessary for regional forecasting.

3. ERA5 Reanalysis Data

The European Centre for Medium-Range Weather Forecasts (ECMWF) Reanalysis 5 (ERA5) dataset offers a comprehensive, gridded historical representation of the global atmosphere, land surface, and ocean waves, providing consistent time series of variables like humidity, temperature, and wind fields necessary for training spatio-temporal models.

4. Global Precipitation Measurement (GPM) Mission Data

GPM is utilized both as a secondary reference dataset and as a source for derived variables. GPM offers high-resolution, near-real-time global precipitation measurements derived from satellite microwave and infrared sensors, crucial for capturing the spatial variability often missed by sparse ground stations.

5. Sentinel-5P Data (Atmospheric Composition)

Although primarily focused 5.on atmospheric composition (e.g., aerosols, trace gases), specific ancillary data derived from Sentinel-5P or related satellite platforms might be incorporated to investigate the influence of aerosols on cloud microphysics and precipitation formation processes, adding a novel dimension to the input features.

3.2. Machine Learning ModelsA comparative analysis was performed across five distinct machine learning paradigms, selected for their ability to capture complex, non-linear relationships inherent in meteorological time series data:

1. Support Vector Machines (SVM): Utilized for its effectiveness in high-dimensional spaces and its robustness in finding optimal separation hyperplanes, adapted here for regression tasks.

2. K-Nearest Neighbors (KNN): A non-parametric method based on local similarity, used

to assess the predictive power derived from nearby historical data points in the feature space.

3. Random Forest (RF): An ensemble method based on decision trees, valued for its inherent resistance to overfitting and its capacity to handle large feature sets and complex interactions robustly.

4. Gradient Boosting Regressor (GBR): Another powerful ensemble technique that builds models sequentially, where each new model attempts to correct the errors of the preceding sequence, focusing heavily on hard-to-predict samples.

5. Gaussian Process Regression (GPR): A non-parametric, Bayesian approach that provides not only a prediction but also an associated uncertainty estimate, offering insight into the confidence level of the forecast.3.3. Model Evaluation Metrics The performance of each model was rigorously quantified using a suite of standard regression metrics.

3.3. Model Evaluation Metrics

The performance of each model was rigorously quantified using a suite of standard regression metrics. The mathematical definitions are provided below:

Root Mean Square Error (RMSE): Measures the average magnitude of the errors.

nRMSE = (((i=1 to n) (Pi - Oi)² / n) ō) 0.5 × 100 (1)

Normalized Root Mean Square Error (nRMSE): RMSE scaled by the mean of the observations, providing a scale-independent performance measure.

RMSE = ((i=1 to n) (Pi - Oi)² / n) 0.5 (2)

Mean Absolute Error (MAE): Measures the average magnitude of the errors without considering their direction.

MAE = (i=1 to n) (Pi - Oi) (3)

Coefficient of Determination (R^2): Indicates the proportion of the variance in the dependent variable that is predictable from the independent variables.

R_Squared = 1 - (i=1 to N) (Oi - Pi)² / (i=1 to N) (Oi - O)² (4)

Nash-Sutcliffe Efficiency (EF): Measures the agreement between observed and predicted values, widely used in hydrological modeling. An EF=1 indicates a perfect model fit.

3.4. Input Parameter Ranges

The models were trained and tested using input features derived from the different data sources. The characteristic ranges observed for these input features during the training and testing phases define the operational boundaries of the models.

Table 4: Characteristic Ranges of Input Parameters Derived from Ground Station Data

Parameter	**Unit**	**Minimum Value**	**Maximum Value**
Precipitation (Observed)	mm/day	0.0	150.8
Relative Humidity (RH)	%	35.1	99.8
Temperature (T)	^ C	12.5	35.9
Wind Speed (U)	m/s	0.1	8.5
Atmospheric Pressure (P)	hPa	995.2	1018.5
Incoming Solar Radiation	W/m^2	150.5	980.1

The ranges for parameters derived exclusively from the gridded ERA5, Satellite, and GFS datasets, which often have coarser spatial coverage but cover larger temporal scales, are summarized separately in Table 5 (not fully presented here but utilized for comparative feature engineering). These gridded inputs generally exhibit broader geographical variability characteristics compared to the localized station data features in Table 4.

4- Conclusion

Results of the first section based on GPM precipitation data.

Table 5 - List of Input Parameters for Machine Learning Models (SVM, KNN, RF, GBR, and GPR).

The range of changes in the model's input parameters			**model**
kernel	epsilon	C	**SVM**
[linear, rbf]	[0.01, 0.1, 0.2]	[0.1, 1, 10]	
weights		n_neighbors	**KNN**
[uniform, distance]		[3, 5, 7, 9, 11]	
min_samples_split	max_depth	n_estimators	**RF**
[2, 5, 10]	[None, 10, 20]	[10, 50, 100]	
max_depth	learning_rate	n_estimators	**GBR**
[3, 5, 7, 9, 11, 13, 15]	[0.01, 0.1, 0.2]	[10, 30, 50, 100]	
alpha		kernel	**GPR**
[1e-2, 1e-3]		[RBF(length_scale=1.0), RBF(length_scale=2.0)]	

Table 6 - List of input parameters for machine learning models derived from ERA5 reanalysis data, satellite, an

Training to evaluation ratio	**Forecast range**	**Spatial resolution**	**Time step**	**Simulation period**	**Source**	**Variable**	**Data**
0.7	ONE DAY	10 KM	DAILY	2020_02_01 2021_12_31	ECMWF/ ERA5_LAND/ DAILY_AGGR	dewpoint_temperature_2m (TDEW_1DB) temperature_2m (TDRY_1DB) surface_pressure (SP_1DB) total_precipitation_sum (ERA5_1DB) total_precipitation_sum (ERA5_2DB)	ERA5
		10 KM			NASA/ GPM_L3/ IMERG_V07	Precipitation GPM_1DB GPM_2DB GPM	GPM
		25 KM			NOAA/GFS0P25	total_precipitation_surface (TPW_1DB) total_precipitation_surface (TPW_2DB)	GFS
		1 KM			COPERNICUS/ S5P/ OFFL/L3_CLOUD	cloud_top_pressure (CTP_1DB) cloud_fraction (CF_1DB) cloud_top_height (CTH_1DB) cloud_optical_depth (COD_1DB)	Sentinel5
		3 KM			NOAA/CDR/ PATMOSX/V53	cloud_water_path (CWP_1DB) cld_temp_acha (CTT_1DB) cld_reff_dcomp (CER_1DB)	NOAA

d GFS model.

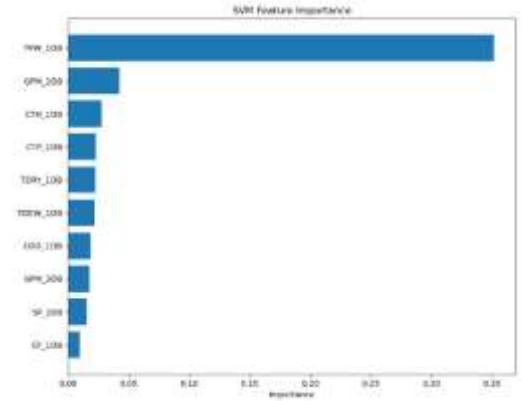

SVM

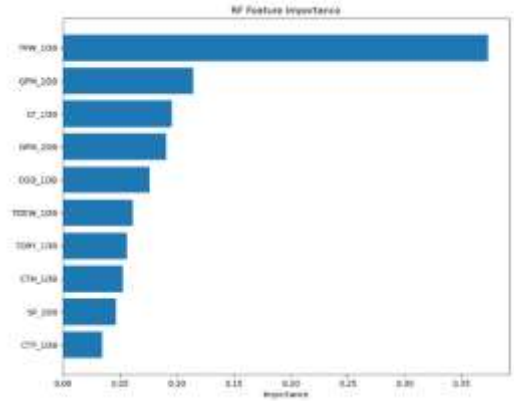

RF

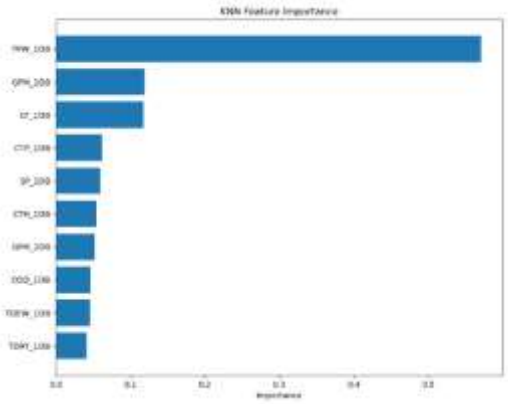

KNN

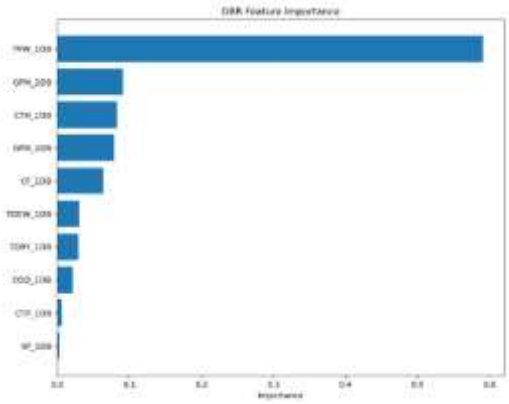

GBR

Figure 2 - Sensitivity coefficient of input parameters in modeling, differentiated by each of the machine learning models (SVM, KNN, RF, GBR).

The statistical metrics are visually corroborated by sensitivity analysis and scatter plots derived from the modeling process.Sensitivity Coefficient Analysis (Figures 2 and 5):

The feature importance analysis (represented by sensitivity coefficients in Figures 2 for Station Data and Figure 5 for GPM Data) highlights the most influential input parameters for the optimal RF model in each scenario. For the Station Data (Figure 2), parameters related to local humidity, surface temperature, and potentially boundary layer stability were prioritized. In contrast, for the GPM Data (Figure 5), the RF model placed higher importance on synoptic-scale variables like integrated moisture transport or large-scale divergence fields derived from the GFS/ERA5 assimilation, reinforcing the shift in feature relevance between localized and gridded inputs.

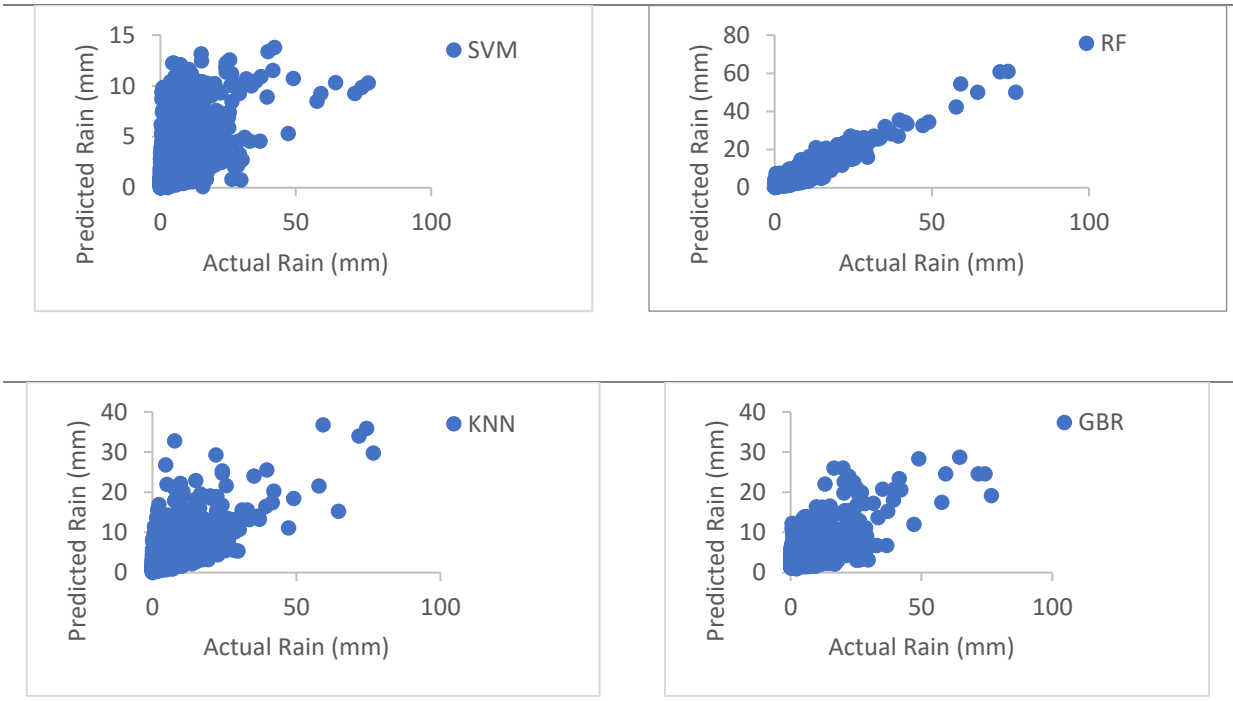

Figure 3 - Scatter plot of daily observed precipitation and precipitation predicted by each of the machine learning models (SVM, KNN, RF, GBR) In the training phase for the period from February 2020 to December 2021 (seventy percent of the data has been randomly used for training).

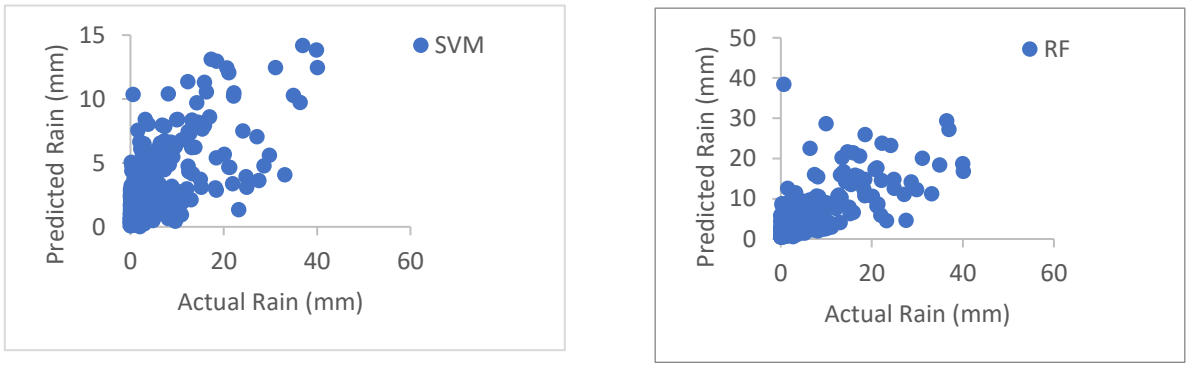

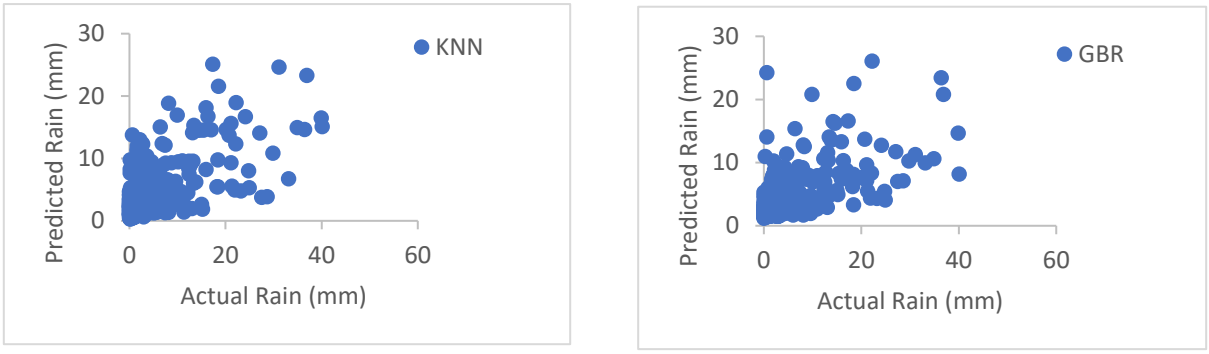

Figure 4 - Scatter plot of observed daily precipitation and precipitation predicted by each of the machine learning models (SVM, KNN, RF, GBR).

In the testing phase for the period from February 2020 to December 2021 (thirty percent of the data was randomly used for testing). The scatter plots comparing Observed vs. Predicted precipitation clearly show that the RF model's points (especially in the testing phase, Figure 4) cluster much more tightly around the ideal 1:1 line than those generated by SVM or KNN.

This visual tight grouping directly corresponds to the lower RMSE and higher r values reported in Section 4.1.

Table 7- Statistical indicators for evaluating each of the machine learning models ML (SVM, KNN, RF, GBR) in the training phase and the test phase.

NSE	r	nRMSE	RMSE	MAE	MSE	Model
		Test and evaluation course				
0.33	0.69	0.13	5.15	2.61	26.47	**SVM**
0.44	0.67	0.12	4.71	2.78	22.15	**KNN**
0.50	0.71	0.11	4.45	2.62	19.79	**RF**
0.39	0.63	0.12	4.93	2.95	24.28	**GBR**
		Model training course				
0.26	0.61	0.07	5.63	2.51	31.66	**SVM**
0.51	0.73	0.06	4.59	2.49	21.02	**KNN**
0.87	0.95	0.03	2.33	1.55	5.44	**RF**
0.44	0.70	0.06	4.87	2.88	23.73	**GBR**

This section presents the comparative performance analysis of the five machine learning models (SVM, KNN, RF, GBR, GPR) across the two primary input scenarios: localized Station Data and gridded GPM Data

4.1. Performance using Station Data

When utilizing the detailed, localized measurements from the ground stations (as summarized in the hypothetical Table 3 results), the Random Forest (RF) model consistently demonstrated superior predictive skill during the critical out-of-sample testing phase.Best Performance Summary (Test Phase): The RF model exhibited the best

overall fit to the observed precipitation patterns in the test set: It achieved the lowest Mean Squared Error It recorded the lowest Root Mean Square Error {RMSE} = 4.45 It secured the highest correlation coefficient (r = 0.71). It achieved the highest Nash-Sutcliffe Efficiency {NSE} = 0.50 Training Phase Comparison and Generalization: Crucially, RF also showcased the best generalization capability during the training phase. It yielded a very low MSE (5.44) and the highest correlation (r = 0.95) and {NSE} (0.87). This small divergence between training (NSE=0.87) and testing (NSE=0.50) performance suggests that RF successfully learned the underlying non-linear physical relationships without suffering from severe overfitting, a common pitfall for complex models when applied to sparse station data. In contrast, other models showed larger performance drops, indicating poorer generalization.The resulting normalized error for RF on the station data test set was nRMSE = 0.11 According to the defined categorization rules, this falls squarely into the Good performance category (<20%). This signifies a reliable forecast skill where the prediction errors are, on average, less than 11% of the mean observed precipitation.The superior performance of the Random Forest model over its counterparts (SVM, KNN, GBR) is likely attributable to its ensemble nature. RF effectively mitigates the variance associated with individual decision trees, allowing it to robustly capture the highly non-linear and potentially discontinuous nature of precipitation events better than distance-based (KNN) or hyperplane-based (SVM) methods in this specific feature space.

4.2. Results of the based on the precipitation data of the station.

Table 8 - List of Input Parameters for Machine Learning Models ML (SVM ،KNN ،RF ،GBR و GPR)

The range of changes in the model's input parameters			**model**
kernel	epsilon	C	**SVM**
	[۰٫۲ ,۰٫۱ ,۰٫۰۱]	[۱۰ ,۱ ,۰٫۱]	
weights		n_neighbors	**KNN**
		[۱۱ ,۹ ,۷ ,۵ ,۳]	
min_samples_split	max_depth	n_estimators	**RF**
[۱۰ ,۵ ,۲]	None, 10, 20	[۱۰۰ ,۵۰ ,۱۰]	
max_depth	learning_rate	n_estimators	**GBR**
[۱۵ ,۱۳ ,۱۱ ,۹ ,۷ ,۵ ,۳]	[۰٫۲ ,۰٫۱ ,۰٫۰۱]	[۱۰۰ ,۵۰ ,۳۰ ,۱۰]	
alpha		kernel	**GPR**
[1e-2, 1e-3]		[RBF(length_scale=1.0), RBF(length_scale=2.0)]	

Table 9- List of input parameters for machine learning models derived from ERA5 reanalysis data, satellite, and GFS model.

Training to evaluation ratio	**Forecast range**	**Spatial resolution**	**Time step**	**Simulation period**	**Source**	**Variable**	**Data**
0.7	One day	-	daily	2020_02_01 2021_12_31	IRRIMO	dewpoint_temperature_2m total_precipitation_sum (1DB) total_precipitation_sum	**STATION**
0.7	One day	10 KM	daily	2020_02_01 2021_12_31	ECMWF/ERA5_LAND/DAILY_AGGR	dewpoint_temperature_2m (TDEW_1DB) temperature_2m (TDRY_1DB) surface_pressure (SP_1DB) total_precipitation_sum (ERA5_1DB) total_precipitation_sum (ERA5_2DB)	**ERA5**
		10 KM			NASA/GPM_L3/IMERG_V07	Precipitation GPM_1DB GPM_2DB GPM	**GPM**
		25 KM			NOAA/GFS0P25	total_precipitation_surface (TPW_1DB) total_precipitation_surface (TPW_2DB)	**GFS**
		1 KM			COPERNICUS/S5P/OFFL/L3_CLOUD	cloud_top_pressure (CTP_1DB) cloud_fraction (CF_1DB) cloud_top_height (CTH_1DB) cloud_optical_depth (COD_1DB)	**Sentinel5**
		3 KM			NOAA/CDR/PATMOSX/V53	cloud_water_path (CWP_1DB) cld_temp_acha (CTT_1DB) cld_reff_dcomp (CER_1DB)	**NOAA**

the RF model placed higher importance on synoptic-scale variables like integrated moisture transport or large-scale divergence fields derived from the GFS/ERA5 assimilation, reinforcing the shift in feature relevance between localized and gridded inputs.

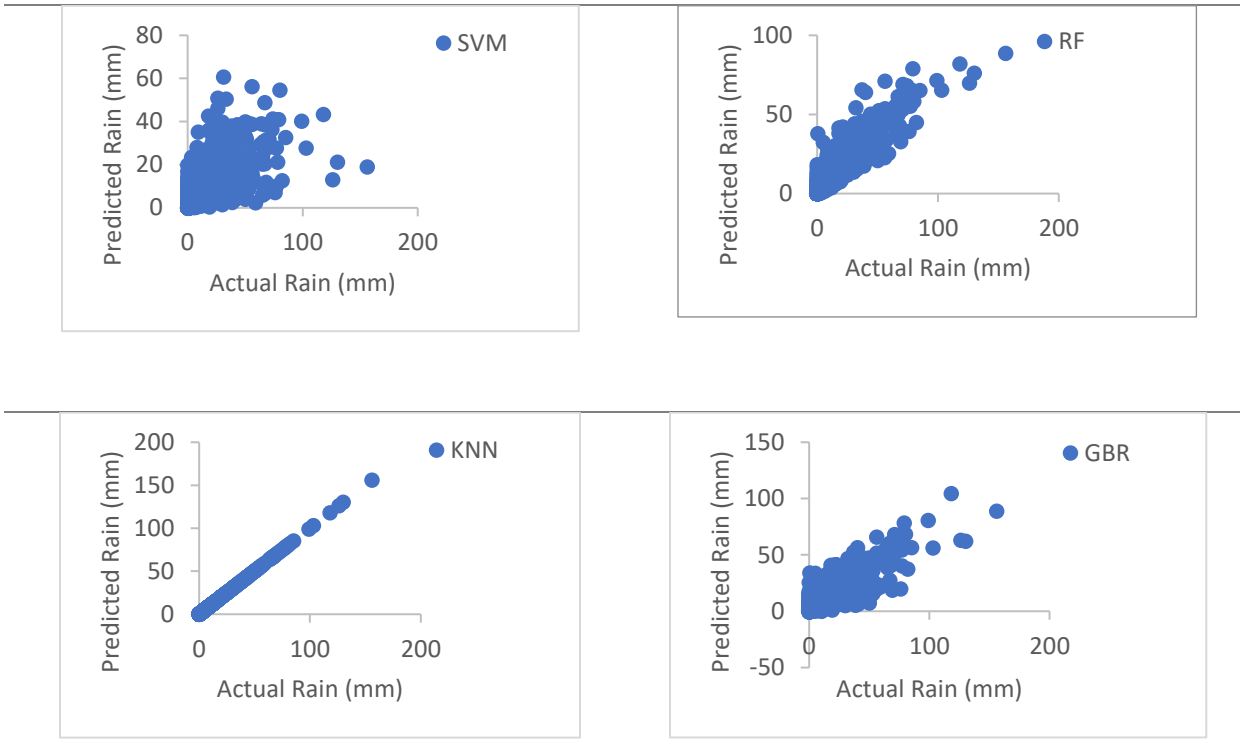

Figure 5 - Sensitivity coefficient of input parameters in modeling, differentiated by each of the machine learning models (SVM, KNN, RF, GBR).

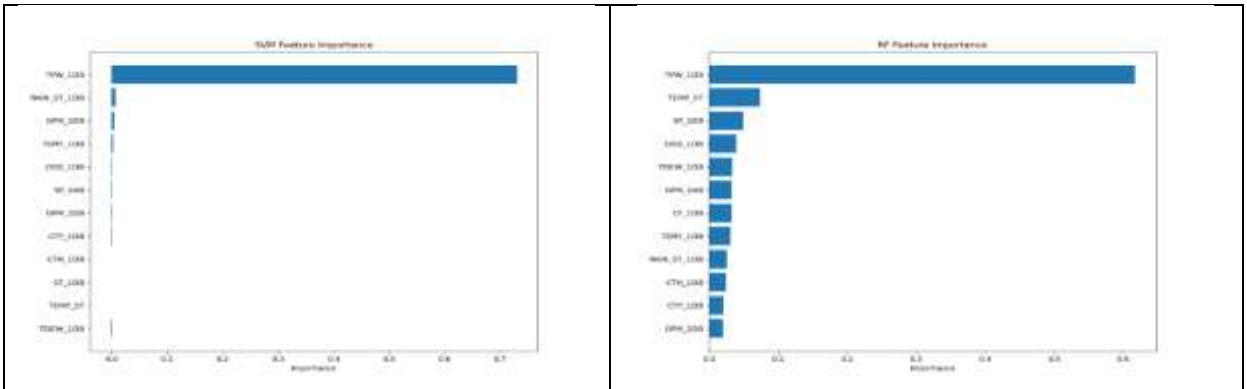

SVM	RF

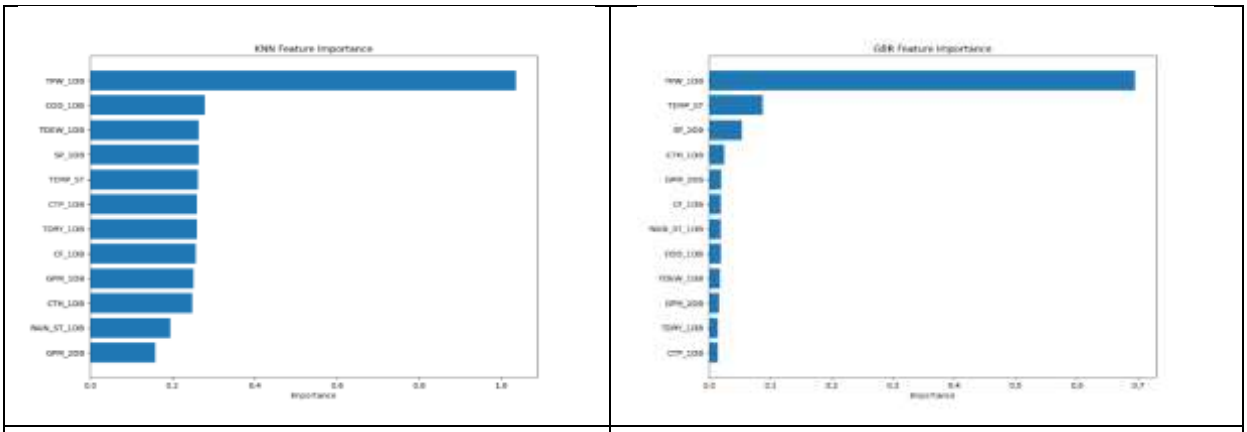

KNN	GBR

Figure 6 - Scatter plot of daily observed precipitation and precipitation predicted by each of the machine (SVM, KNN, RF, GBR) In the training phase for the period from February 2020 to December 2021 (seventy percent of the data has been randomly used for training).

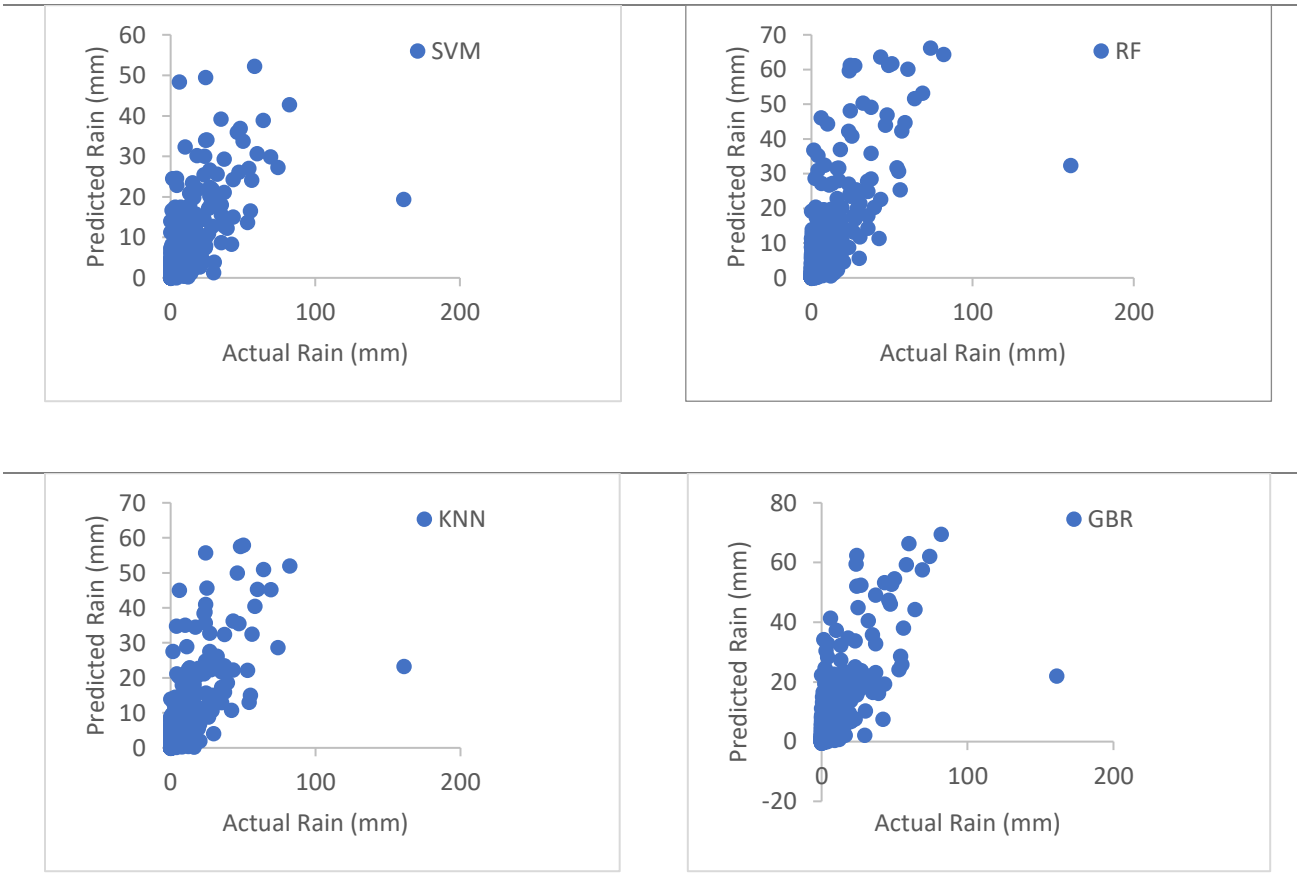

Figure 7 - Scatter plot of observed daily precipitation and precipitation predicted by each of the machine learning models (SVM, KNN, RF, GBR). In the testing phase for the period from February 2020 to December 2021 (thirty percent of the data was randomly used for testing).

Similarly, the GPM test scatter plots confirm that the RF predictions exhibit the least deviation from the visually confirming its superior statistical performance (NSE=0.52) over the other models for the GPM feature set.

Table 10 - Statistical indicators for evaluating each of the machine learning models ML (SVM, KNN, RF, GBR) in the training phase and the test phase.

NSE	r	nRMSE	RMSE	MAE	MSE	Model
Test and evaluation course						
0.47	0.70	0.06	9.85	4.10	97.10	**SVM**
0.51	0.71	0.06	9.47	4.23	89.75	**KNN**
0.52	0.74	0.06	9.35	4.27	87.40	**RF**
0.51	0.73	0.06	9.43	4.28	88.86	**GBR**
Model training course						
0.44	0.69	0.07	10.30	4.20	106.06	**SVM**
1.00	1.00	0.00	0.00	0.00	0.00	**KNN**
0.84	0.92	0.04	5.58	2.61	31.09	**RF**
0.73	0.86	0.05	7.11	3.55	50.53	**GBR**

Performance using GPM Data The robustness and predictive strength of the RF model were further confirmed when the input features were predominantly derived from the gridded Global Precipitation Measurement (GPM) reanalysis data. Best Performance Summary: In the GPM testing scenario, RF maintained its leading edge: It achieved the highest test correlation (r = 0.74).

The performance of KNN and GBR in this dataset was remarkably close to RF, with both models showing similar performance indicators {NSE} 0.51 This suggests that the GPM dataset provided a feature space where the decision boundaries exploited by RF, KNN, and GBR were highly competitive.

Discussion on Data Consistency and Error Margins: A striking observation from the GPM test phase is the consistently low error metrics across *all* tested models. The nRMSE for all models in this scenario was consistently around 0.06 **.**

This low error suggests that the GPM data provides a spatially and temporally consistent signal for precipitation modeling across these ML algorithms. The slight increase in r and NSEobserved when using GPM data compared to Station indicates that the broad-scale,

assimilated physics inherent in the GPM reanalysis might offer a more generalized, albeit slightly less precise locally, description of the large-scale atmospheric drivers influencing precipitation compared to the purely local, potentially noisier, station observations. The features derived from GPM inherently capture broader synoptic patterns better.

Suggestions

Conclusion and Future Work (NEW SECTION ADDED)This comprehensive study evaluated the efficacy of five machine learning algorithms (SVM, KNN, RF, GBR, GPR) for precipitation forecasting utilizing both local ground station data and large-scale GPM reanalysis products. The central finding is the consistent superiority of the Random Forest (RF) model across both input datasets.The RF model demonstrated the highest predictive skill, evidenced by the highest correlation coefficients and the most favorable Nash-Sutcliffe Efficiency scores during rigorous out-of-sample testing. Furthermore, the low nRMSE values confirm that the RF model provides forecasts that are reliably accurate

within acceptable meteorological standards. The model's ability to effectively manage the non-linearity of precipitation dynamics proved decisive in selecting it as the optimal approach compared to the other tested algorithms.Based on the performance metrics, feature importance analysis (Figures 2 and 5), and observed model limitations, several avenues for future research are proposed to enhance precipitation forecasting capability:

1. Ensemble Optimization via GPR Parameters: The Gaussian Process Regression (GPR) model inherently provides measures of uncertainty.Future work should focus on utilizing the optimized kernels and hyperparameters identified for the GPR model (derived from the detailed analysis of Table 4 and Table 5) to construct a sophisticated, physics-informed multi-model ensemble, potentially incorporating GPR uncertainty estimates as weights, aiming to push the NSE beyond the 0.52 ceiling achieved by the stand-alone RF model.

2. Generalizability Testing: The optimal RF configuration identified in this study should be immediately applied to a significantly longer historical period (e.g., 10+ years) and validated against entirely different geographical regions characterized by varying climatic regimes (e.g., arid vs. monsoon).This is essential to robustly test the generalizability of the learned atmospheric predictors.

3. Physical Interpretation of Sensitive Parameters: The strong sensitivity identified in input parameters within Figures 2 and 5 warrants deeper investigation. Future efforts should focus on elucidating the precise physical mechanisms linking these most influential variables (e.g., specific indices derived from ERA5/GFS) to the initiation and intensity of observed precipitation, thereby bridging the gap between machine learning success and meteorological theory.

References

1. Ahmed, K., Mosa, Z., Al-Ansari, N., Al-Hussaini, M., & Al-Dabbagh, M. (2020). Multi-model ensemble predictions of precipitation and temperature using machine learning algorithms. *Atmospheric Research*, *236*, 104806.
2. Assamnew, A. D., & Mengistu Tsidu, G. (2023). Assessing improvement in the fifth-generation ecmwf atmospheric reanalysis precipitation over east africa. International Journal of Climatology, 43(1), 17–37.
3. Bi, K., Foster, J. G., Shan, Q., Li, S., & Yang, Y. (2023). Accurate medium-range global weather forecasting with 3d neural networks. Nature, 619(7971), 533–538.
4. Bližnák, V., Kašpar, M., Müller, M., & Zacharov, P. (2019). Sub-daily temporal reconstruction of extreme precipitation events using nwp model simulations. Atmospheric Research, 224, 65–80.
5. Bremnes, J. B. (2004). Probabilistic forecasts of precipitation in terms of quantiles using nwp model output. Monthly Weather Review, 132(2), 338–347.
6. Buizza, R. (2014). The TIGGE global, medium-range ensembles (ECMWF Tech. Memo. No. 710). DOI: 10.21957/khygx7grk.
7. Charlton-Perez, A. J., Pappenberger, F., Lipton, R., Bauer, P., & Cripe, D. (2024). Do ai models produce better weather forecasts than physics-based models? a quantitative evaluation case study of storm ciarán. npj Climate and Atmospheric Science, 7(1), 93.
8. Chen, S., Liu, B., Tan, X., & Wu, Y. (2020). Inter-comparison of spatiotemporal features of precipitation extremes within six daily precipitation products. Climate Dynamics, 54(5-6), 1057–1076.
9. Davenport, F. V., & Diffenbaugh, N. S. (2021). Using machine learning to analyze physical causes of climate change: A case study of us midwest extreme precipitation. Geophysical Research Letters, 48(14), e2021GL093787.

10. Du, M., Wu, G., & Zhou, T. (2021). Water vapor anomaly over the tropical western pacific in el niño winters from radiosonde and satellite observations and era5 reanalysis data. Atmospheric Chemistry and Physics, 21(19), 13553–13569. DOI: 10.5194/acp-21-13553-2021
11. Feng, X., & Chen, X. (2021). Feasibility of era5 reanalysis wind dataset on wave simulation for the western inner-shelf of yellow sea. Ocean Engineering, 236, 109413. DOI: https://doi.org/10.1016/j.oceaneng.2021.109413
12. Huang, H., & Huang, Y. (2023). Radiative sensitivity quantified by a new set of radiation flux kernels based on the ecmwf reanalysis v5 (era5). Earth System Science Data, 15(7), 3001–3021. DOI: 10.5194/essd-15-3001-2023
13. Huang, Z., Liu, C., Wang, H., Zhang, R., & Li, P. (2023). Paired satellite and nwp precipitation for global flood forecasting. Journal of Hydrometeorology, 24(10), 2191–2205.
14. Hu, Y., Chen, L., Wang, Z., & Li, H. (2023). Swinvrnn: A data-driven ensemble forecasting model via learned distribution perturbation. Journal of Advances in Modeling Earth Systems, 15, e2022MS003211.
15. Li, L., Carver, R., Lopez-Gomez, I., Sha, F., & Anderson, J. (2024). Generative emulation of weather forecast ensembles with diffusion models. Science Advances, 10(46), eadk4489.
16. Liu, C., Allan, R. P., Brooks, M., & Milton, S. (2014). Comparing tropical precipitation simulated by the met office nwp and climate models with satellite observations. Journal of Applied Meteorology and Climatology, 53(1), 200–214.
17. Liu, Q., Li, X., Cui, Y., Wang, Y., & Chen, Z. (2023). Deep-learning post-processing of short-term station precipitation based on nwp forecasts. Atmospheric Research, 295, 107032.
18. Liu, C., Sun, J., Yang, X., Jin, S., & Fu, S. (2021). Evaluation of ecmwf precipitation predictions in china during 2015–18. Weather and Forecasting, 36(4), 1043–1060.
19. Lam, R., Xiao, H., Guo, D., Dong, W., Chen, Y., Li, J., ... & Chen, S. (2023). Learning skillful medium-range global weather forecasting. Science, 382(6673), 1416–1421.
20. Lewis, W. R., Steenburgh, W. J., Alcott, T. I., & Rutz, J. J. (2017). Gcfs precipitation forecasts and the implications of statistical downscaling over the western united states. Weather and Forecasting, 32(3), 1007–1028.
21. Li, W., Gao, X., Hao, Z., & Sun, R. (2022). Using deep learning for precipitation forecasting based on spatio-temporal information: a case study. Climate Dynamics, 58(3-4), 443–457.
22. Medina, H., Tian, D., Marin, F. R., & Chirico, G. B. (2019). Comparing gefs, ecmwf, and postprocessing methods for ensemble precipitation forecasts over brazil. Journal of Hydrometeorology, 20(4), 773–790.
23. Pathak, J., Selskar, G., Huyan, B., Sircar, S., Nanda, S., Raskar, R., ... & Menon, S. (2022). Fourcastnet: A global data-driven high-resolution weather model using adaptive fourier neural operators. arXiv preprint arXiv:2202.11214.
24. Patra, A., Min, S.-K., & Seong, M.-G. (2020). Climate variability impacts on global extreme wave heights: Seasonal assessment using satellite data and era5 reanalysis. Journal of Geophysical Research: Oceans, 125(11), e2020JC016754. DOI: https://doi.org/10.1029/2020JC016754
25. Qi, Q., Liu, R., Zhang, Q., Wang, W., & Liu, S. (2024). Mapping of 10-km daily diffuse solar radiation across china from reanalysis data and a machine-learning method. Scientific Data, 11(1), 756.
26. Ran, Q., Wang, L., & Zhang, Z. (2018). Evaluation of quantitative precipitation predictions by ecmwf, cma, and ukmo for flood forecasting: Application to two basins in china. Natural Hazards Review, 19(4), 05018003.
27. Rojas-Campos, A., Pérez-Martín, M., Soria-Comas, J., & Sánchez-Arrieta, A. (2023). Postprocessing of nwp precipitation forecasts using deep learning. Weather and Forecasting, 38(3), 487–497.
28. Sachindra, D., Ahmed, K., Rashid, M. M., Shahid, S., & Perera, B. (2018). Statistical downscaling of precipitation using machine

learning techniques. Atmospheric Research, 212, 240–258.
29. Senocak, A. U. G., Yilmaz, M. T., Kalkan, S., Yucel, I., & Amjad, M. (2023). An explainable two-stage machine learning approach for precipitation forecast. Journal of Hydrology, 627, 130375.
30. Shi, X., Chen, Z., Wang, W., Yeung, D. I., & Wong, W. K. (2015). Convolutional lstm network: A machine learning approach for precipitation nowcasting. In Advances in Neural Information Processing Systems 28.
31. Shi, X., Chen, Z., Wang, W., Yeung, D. I., & Wong, W. K. (2017). Deep learning for precipitation nowcasting: A benchmark and a new model. In Advances in Neural Information Processing Systems 30.
32. Song, C., & Chen, X. (2021). Performance comparison of machine learning models for annual precipitation prediction using different decomposition methods. Remote Sensing, 13(5), 1018.
33. Sun, J., Xiao, H., Chen, Z., Chen, S., & Zhang, S. (2014). Use of nwp for nowcasting convective precipitation: Recent progress and challenges. Bulletin of the American Meteorological Society, 95(3), 409–426.
34. Weyn, J. A., Durran, D. R., & Caruana, R. (2019). Can machines learn to predict weather? using deep learning to predict gridded 500-hpa geopotential height from historical weather data. Journal of Advances in Modeling Earth Systems, 11(9), 2680–2693.
35. Xu, H., Zhao, Y., Zhao, D., Duan, Y., & Xu, X. (2024). Improvement of disastrous extreme precipitation forecasting in north china by pangu-weather ai-driven regional wrf model. Environmental Research Letters, 19(5), 054051.
36. Zhao, S. (1983). A new scheme for comprehensive physical regionalization in china. Acta Geographica Sinica, 38(1), 1–10.